THE JOURNAL OF PHYSICAL CHEMISTRY B

Article

pubs.acs.org/JPCB

Site Specific Interaction of the Polyphenol EGCG with the SEVI Amyloid Precursor Peptide PAP(248−286)

Nataliya Popovych,[†,‡] Jeffrey R. Brender,[†,‡] Ronald Soong,[†,‡] Subramanian Vivekanandan,[†,‡] Kevin Hartman,[†] Venkatesha Basrur,[§] Peter M. Macdonald,[∥] and Ayyalusamy Ramamoorthy*[,†,‡]

[†]Department of Chemistry and [‡]Biophysics, University of Michigan, Ann Arbor, Michigan 48109-1055, United States

[§]Proteomics Resource Facility, Department of Pathology, University of Michigan, United States

[∥]Department of Chemical & Physical Sciences, University of Toronto at Mississauga, Mississauga, Canada

Supporting Information

ABSTRACT: Recently, a 39 amino acid peptide fragment from prostatic acid phosphatase has been isolated from seminal fluid that can enhance infectivity of the HIV virus by up to 4−5 orders of magnitude. PAP(248−286) is effective in enhancing HIV infectivity only when it is aggregated into amyloid fibers termed SEVI. The polyphenol EGCG (epigallocatechin-3-gallate) has been shown to disrupt both SEVI formation and HIV promotion by SEVI, but the mechanism by which it accomplishes this task is unknown. Here, we show that EGCG interacts specifically with the side chains of monomeric PAP(248−286) in two regions (K251−R257 and N269−I277) of primarily charged residues, particularly lysine. The specificity of interaction to these two sites is contrary to previous studies on the interaction of EGCG with other amyloidogenic proteins, which showed the nonspecific interaction of EGCG with exposed backbone sites of unfolded amyloidogenic proteins. This interaction is specific to EGCG as the related gallocatechin (GC) molecule, which shows greatly decreased antiamyloid activity, exhibits minimal interaction with monomeric PAP(248−286). The EGCG binding was shown to occur in two steps, with the initial formation of a weakly bound complex followed by a pH dependent formation of a tightly bound complex. Experiments in which the lysine residues of PAP(248−286) have been chemically modified suggest the tightly bound complex is created by Schiff-base formation with lysine residues. The results of this study could aid in the development of small molecule inhibitors of SEVI and other amyloid proteins.

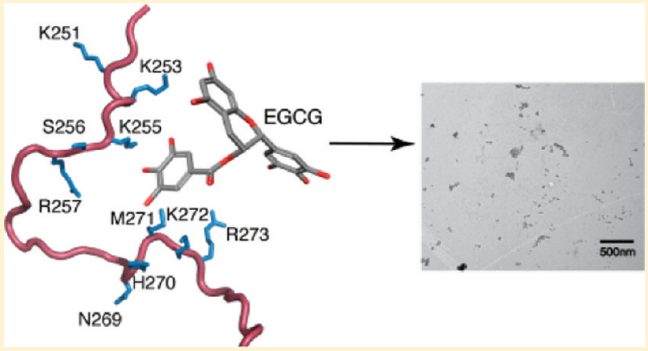

INTRODUCTION

The HIV virus responsible for AIDS is the source of a global pandemic with over 33 million people worldwide currently infected with the virus. The scope of AIDS pandemic sparks the question: why is HIV so prevalent in the population and transmitted so readily *in vivo*, while the virus itself has a very poor infection rate *in vitro*? One possibility is the presence of *in vivo* cofactors that facilitate entry of the virus, causing infection to occur at a higher rate.[1,2] Recently, a cofactor has been found in human seminal fluid that could prove to be a key component in HIV transmission.[3] A peptide fragment of prostatic acid phosphatase ($PAP_{248-286}$, sequence GIHKQKEKSRLQGGVLVNEILNHMKRATQIPSYKKLIMY) was discovered to increase the infection rate of HIV[3−7] and other enveloped viruses[7,8] by several orders of magnitude when aggregated into amyloid fibrils termed SEVI (semen-derived enhancer of viral infection).

The degree to which $PAP_{248-286}$ promotes HIV infection is dependent on the conformation and aggregation state of the peptide, with the monomeric peptide being ineffective at promoting HIV infection.[3,9] Since $PAP_{248-286}$ is only effective in enhancing HIV infection in the aggregated SEVI form, molecules that suppress fibrillization of $PAP_{248-286}$ into the active amyloid form can decrease the effective infectiousness of the HIV virus.[10,11] Given the potentially high impact SEVI amyloid formation may have on the sexual transmission of HIV, a low cost SEVI inhibitor incorporated into an antiretroviral microbicide may have a substantial effect on the HIV transmission rates.[6,11,12]

A polyphenolic compound found in green tea (epigallocatechin-3-gallate or EGCG) inhibits the formation of SEVI fibers, disaggregates existing SEVI fibers, and blocks the SEVI mediated attachment of HIV virion to target cells and SEVI promotion of HIV infectivity.[12] Polyphenolic compounds are among the most effective antiaggregative agents discovered to date, effectively inhibiting aggregation of a broad spectrum of amyloidogenic proteins.[13] The exact mechanism by which

Received: December 16, 2011
Revised: February 23, 2012
Published: February 23, 2012

   dx.doi.org/10.1021/jp2121577 | *J. Phys. Chem. B* 2012, 116, 3650−3658

polyphenols disrupt amyloid formation is unclear, but they appear to act at multiple points along the aggregation pathway to inhibit the elongation of existing fibers and to disrupt the formation of nuclei for further amyloid formation.[14−17] EGCG has been proposed to bind to backbone sites exposed in the disordered conformation of the monomeric species of many amyloid proteins, redirecting the aggregation pathway to amorphous aggregates that are nontoxic and do not share many of the common features of amyloid-based structures.[14,16] The general mechanism by which polyphenolic compounds block amyloid formation is of considerable importance, as amyloid formation is a common feature of many degenerative diseases including Alzheimer's, type II diabetes, Parkinson's, Creutzfield-Jacob's, Huntington's, and others.[18] Small molecules that disrupt aggregated forms of these proteins could have considerable clinical application, making a determination of the mechanism by which polyphenols disrupt aggregated conformations essential for structure−activity assays. EGCG itself has been shown to suppress both amyloid formation and associated toxicity for many of these proteins.[14,16,19−21]

To determine the mechanism by which EGCG disrupts SEVI amyloid formation from its precursor $PAP_{248-286}$, we analyzed binding of EGCG and the related catechin GC (chemical structures shown in Figure 1) to monomeric and small oligomeric

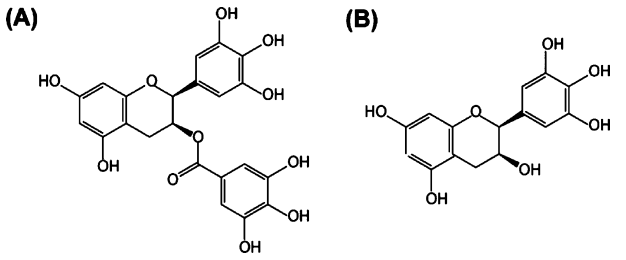

Figure 1. Chemical structures of EGCG (A) and GC (B).

forms of $PAP_{248-286}$ by NMR and other biophysical methods. We show that, contrary to the proposed general mechanism,[14] EGCG interacts specifically with the side chains of $PAP_{248-286}$. Binding occurs by a two-step mechanism in which a weakly bound complex is initially formed from monomeric $PAP_{248-286}$ that is transformed in a pH dependent manner into a covalently cross-linked complex over time following the oxidation of the Met residue. The mechanism proposed in this study suggests the binding of polyphenols to amyloidogenic proteins is more complex than previously proposed and multiple interactions must be considered.

MATERIALS AND METHODS

Sample Preparation. $PAP_{248-286}$ obtained from Biomatik (Toronto, Ontario) was first disaggregated using a TFA (trifluoroacetic acid)/HFIP (hexafluoroisopropanol) mixture and lyophilized as described in ref 38 for all experiments. EGCG ((−)-epigallocatechin-3-gallate) and GC ((−)-gallocatechin) were purchased from Sigma. Stock solutions of EGCG and GC (50 and 30 mM, respectively) were prepared in water and used immediately.

Thioflavin T Fluorescence. The kinetics of $PAP_{248-286}$ amyloid formation in the absence of EGCG or GC was measured by monitoring the increase in fluorescence intensity upon binding of the amyloid fiber to the amyloid specific dye thioflavin T (ThT). Before the start of the experiment, $PAP_{248-286}$ was solubilized in buffers containing 50 mM KPi and 25 μM ThT at two different pH values (pH 7.3 and 6.0) to achieve a final peptide concentration of 439 μM (2 mg/mL). All buffers were filtered and degassed before usage. Experiments were performed in sealed Corning 96 well clear bottom half area, nonbinding surface plates. Time traces were recorded with a Biotek Synergy 2 plate reader using a 440 nm excitation filter and a 485 nm emission filter at a constant temperature of 37 °C with shaking.

Transmission Electron Microscopy (TEM). For inhibition experiments using monomeric $PAP_{248-286}$ solutions at pH 6.0 or 7.3 as a starting point, $PAP_{248-286}$ and EGCG or GC were coincubated for 7 days at 37 °C with linear agitation of the sample at 1500 rpm, using a $PAP_{248-286}$ concentration of 439 μM and a 1:5 molar ratio of EGCG or GC. After incubation, 10 μL aliquots were loaded onto Formvar-coated copper grids (Ernest F. Fullam, Inc., Latham, NY) for 2 min, washed twice with 10 μL of deionized water, and then negatively stained for 90 s with 2% uranyl acetate. Samples were imaged with a Philips CM10 Transmission Electron Microscope at 8400×, 11000×, and 15000× magnification.

For disaggregation experiments, 439 μM $PAP_{248-286}$ was incubated alone for 4 days at 37 °C at pH 6 or 7.3 as described above. After 4 days (pH 7.3) or 8 days (pH 6.1), EGCG or GC was added to the sample in a 1:5 molar ratio and coincubated with the resulting SEVI amyloid fibers for 4 h. The resulting solution was then stained and imaged as described above. A comparison to control grids in the absence of EGCG or GC confirmed the presence of amyloid fibers.

NMR Spectroscopy. NMR samples were prepared by dissolving 0.5 mg of lyophilized peptide in 50 mM phosphate buffer at either pH 6.0 or 7.3 containing 10% D_2O. The peptide concentration was determined from the absorbance at 276 nm and was in the range 0.3−0.4 mM for each sample.

NMR spectra were recorded at 42 °C on a 900 MHz Bruker Avance NMR spectrometer equipped with a triple-resonance *z*-gradient cryogenic probe optimized for ^{1}H-detection. All spectra were processed using TopSpin 2.1 software (Bruker) and analyzed using SPARKY.[22] Binding experiments were performed by titration of the sample from a concentrated EGCG or GC stock solution to a 1:1 molar ratio. Backbone and side chain assignments were performed using 2D ^{1}H−^{1}H TOCSY (total correlation spectroscopy) and 2D ^{1}H−^{1}H NOESY (nuclear Overhauser enhancement spectroscopy) recorded at two different mixing times 70 or 80 and 300 ms, respectively. Complex data points were acquired for quadrature detection in both frequency dimensions in 2D experiments, and all the spectra were zero-filled in both dimensions to yield matrices of 2048 × 2048 points. Resonance assignments have been deposited in the Biological Magnetic Resonance Bank (BMRB) database (accession number is 18287).

Proton diffusion NMR measurements were carried out at 499.78 MHz using the stimulated echo (STE) pulsed field gradient (PFG) pulse sequence with squared gradient pulses of constant duration (5 ms) and a variable gradient amplitude along the longitudinal axis.[23] To assay possible time-dependent aggregation behavior, the PFG-NMR experiment was repeated every 2 h on each sample for a total of 12 h. Other parameters used in NMR experiments were as follows: a 90° pulse width of 23 μs, a spin−echo delay of 10 ms, a stimulated-echo delay of 150 ms, a recycle delay of 5 s, a spectral width of 10 kHz, and 4048 data points. A saturation pulse centered at the water ^{1}H resonance frequency was used for solvent suppression.

dx.doi.org/10.1021/jp2121577 | J. Phys. Chem. B 2012, 116, 3650−3658

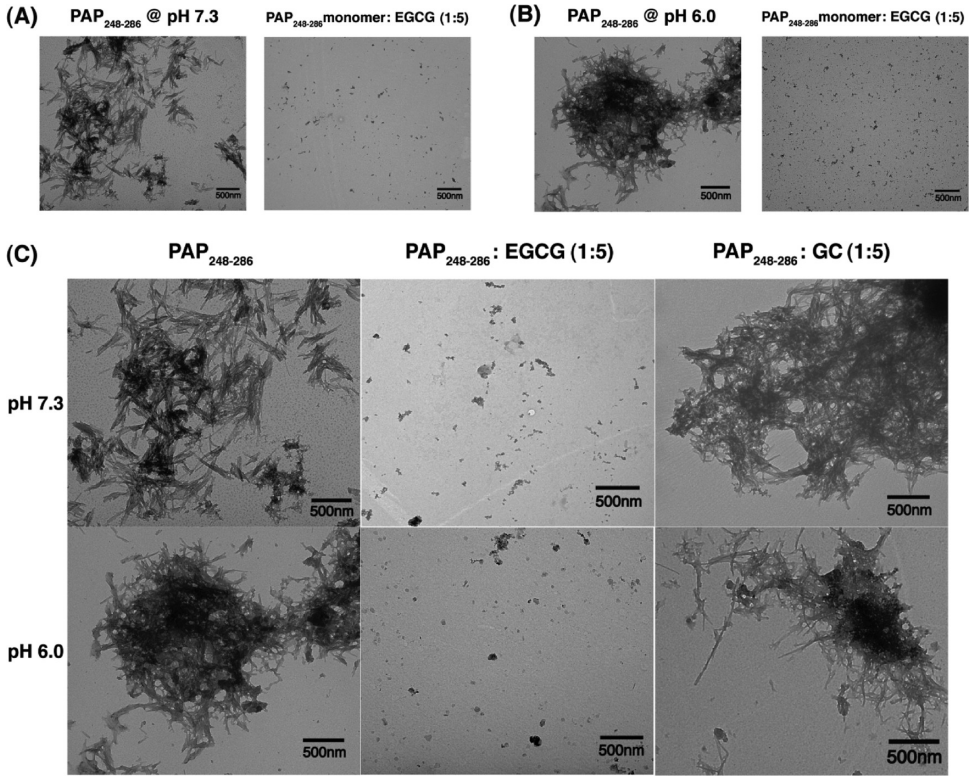

Figure 2. EGCG inhibits SEVI formation from $PAP_{248-286}$ and disaggregates existing fibers while the related catechin GC has a diminished effect. (A) TEM image of $PAP_{248-286}$ incubated alone for 4 days (left) and coincubated for 4 days with EGCG at a 1:5 molar ratio (right) at pH 7.3. (B) As above but for 7 days incubation at pH 6. (C) TEM images of existing SEVI amyloid fibers (left), SEVI amyloid fibers coincubated with EGCG for 5 h (1:5 molar ratio) (center), and coincubated with GC for 5 h (1:5 molar ratio) (right).

Radio frequency pulses were phase cycled to remove unwanted echoes. All spectra were processed with a 5 Hz exponential line broadening prior to Fourier transformation and were referenced relative to 4,4-dimethyl-4-silapentane-1-sulfonic acid (DSS at 0 ppm). The gradient strength was calibrated (G = 3.28 T m^{-1}) from the known diffusion coefficient of HDO in D_2O at 25 °C ($D_0 = 1.9 \times 10^{-9}$ m^2 s^{-1}).[24] The diffusion coefficients were determined from the slope of a log plot of the intensity as a function of gradient strength using the Stejskal–Tanner equation.[25] The hydrodynamic radius was then calculated from the diffusion coefficient using the Einstein–Stokes relation.

SDS-PAGE and NBT (Nitroblue Tetrazolium) Staining. $PAP_{248-286}$ peptide alone and complexes of $PAP_{248-286}$ with EGCG and GC in a 1:5 molar ratio were incubated at the times, temperatures, and solutions indicated below and then analyzed by SDS-PAGE on 17% acrylamide gels using Comassie blue staining. A 360 μM concentration of $PAP_{248-286}$ was used. The same samples were also analyzed by NBT staining to detect protein-bound EGCG quinines.[26] For NBT staining, proteins were first separated by SDS-PAGE gel and electroblotted onto nitrocellulose membrane. The membrane was then stained with glycinate/NBT solution (0.24 mM nitroblue tetrazolium in 2 M potassium glycinate, pH 10.0) for 1 h in the dark. This resulted in a purple stain of quinone-bound protein bands. The membrane was washed and stored in 0.1 M sodium borate (pH 10.0).

Blocking ϵ-NH_2 of Lysine in $PAP_{248-286}$ Using Acetic Anhydride. $PAP_{248-286}$ peptide was first dissolved in 50 mM borate buffer (pH 8.0), and then, an equimolar amount of acetic anhydride was added to the peptide solution.[27] The sample was then mixed with EGCG in a 1:5 molar ratio and preincubated at room temperature for 2–3 h before the NBT assay.

Mass Spectrometry Analysis. Samples of $PAP_{248-286}$ for mass spectrometry analysis were first incubated at a concentration of 50 μM with EGCG at a 1:5 molar ratio for 3 days at room temperature in ammonium acetate buffer (10 mM, pH 6 or 7.3) before analysis. $PAP_{248-286}$ by itself was used as a control. Mass spectra were obtained using an Orbitrap XL (ThermoFisher) electrospray-ionization (ESI) mass spectrometer. All samples were directly injected into the ESI source in positive ion mode using a flow rate of 3 μL/min. The source temperature was set to 250 °C and the electrospray voltage to 4.5 kV. Before starting the experiment, the instrument was calibrated with standard compounds (per instrument manufacturer's specification). Mass spectra were acquired continuously for 1 min, and peaks between 400 and 2000 m/z were processed by BioworksBrowser (3.3.1 SP1, ThermoFisher) software.

RESULTS

EGCG but Not GC Inhibits SEVI Formation at Neutral and Acidic pH. Hauber et al. showed that an excess of EGCG inhibits SEVI amyloid formation from $PAP_{248-286}$ and slowly disaggregates existing SEVI fibers.[12] These experiments were performed at pH 7.3; however, a likely microbicide containing an anti-SEVI inhibitor would have to be effective in the vaginal environment where the pH is significantly acidic, with a pH closer to 6 than 7.3.[28] $PAP_{248-286}$ has two histidine residues that are likely to have pK_a values in this range, which may in turn effect fiber formation and/or EGCG binding. It has previously been shown that a strongly acidic environment (2% acetic acid)

dx.doi.org/10.1021/jp2121577 | J. Phys. Chem. B 2012, 116, 3650–3658

maintains the peptide in a monomeric state, but the effect of a moderately acidic environment on SEVI fiber formation and EGCG binding is not known.[29] We therefore first tested to see if EGCG would be effective at inhibiting the peptide $PAP_{248-286}$ aggregation in an acidic environment (pH 6) as it is in a neutral environment (pH 7.3).

To test the aggregation kinetics, we first used the commonly used amyloid specific dye thioflavin T (ThT). Thioflavin T is a benzothiazole salt whose fluorescence is enhanced when it binds to grooves in the amyloid fiber running parallel to the fiber axis. As measured by ThT fluorescence, $PAP_{248-286}$ fibrillizes within 53−62 h at pH 7.3 in the absence of EGCG. $PAP_{248-286}$ aggregated more slowly in the absence of EGCG at pH 6 than at pH 7.3 (Figure S1A in the Supporting Information), although faster than in 2% acetic acid,[29] most likely due to the greater electrostatic repulsion between peptides at pH 6 from the additional charge on the two histidine residues. Addition of either EGCG or GC at a 5:1 molar ratio abolishes the increase in thioflavin T fluorescence (Figure S1A, Supporting Information), suggesting both compounds apparently inhibit fiber formation. Addition of EGCG and GC to preformed fibers gives an apparent dissolution half-life of 12 h (Figure S1B, Supporting Information), similar to previously reported values.[12]

However, thioflavin T fluorescence is known to give false positives for inhibition of fiber formation for compounds that competitively bind to the thioflavin T binding site on the amyloid fiber without causing disaggregation of the fiber.[30−32] To confirm the thioflavin T results, transmission electron micrographs (TEM) were taken of $PAP_{248-286}$ after a 96 h incubation period. In the absence of either EGCG or GC, $PAP_{248-286}$ fibrillizes to form a dense network of amyloid fibers (Figure 2A). Coincubation of the $PAP_{248-286}$ monomer with EGCG prevents the formation of this fiber network at both pH 6 and pH 7.3, confirming EGCG actually inhibits fiber formation. Examination of TEM images of preformed $PAP_{248-286}$ fibers incubated with EGCG yields a similar result, confirming EGCG can also dissolve preformed $PAP_{248-286}$ amyloid fibers.

Comparison of the ThT and TEM results for $PAP_{248-286}$ incubated with GC yields a markedly different result. While the ThT signal decreases significantly in the presence of GC, TEM images clearly show GC neither prevents fibers from forming nor dissolves preformed fibers of $PAP_{248-286}$ (Figures S2 (Supporting Information) and 2C, respectively). In this case, the decrease in ThT fluorescence is a false positive for inhibition of fiber formation by GC. In summary, EGCG inhibited aggregation of $PAP_{248-286}$ and disaggregated existing SEVI fibers at both pH 6 and 7.3. By contrast, the addition of the related catechin GC in a 1:5 $PAP_{248-286}$ to GC molar ratio did neither (Figure 2C and Figure S2 (Supporting Information)), in agreement with a previous report showing the absence of amyloid degradation when GC was incubated with SEVI and the lack of an inhibitory action on viral infectivity in the presence of GC.[12]

EGCG Oligomerizes $PAP_{248-286}$ Immediately at pH 7.3 but Not pH 6. Previous reports of the interaction of EGCG with other amyloidogenic proteins have shown the formation of off-pathway oligomers is an important mechanism for the inhibition of amyloid formation by EGCG.[33] To determine if EGCG binding similarly catalyzes the oligomerization of $PAP_{248-286}$, we examined the hydrodynamic radii of the $PAP_{248-286}$ /EGCG complex (1:1 molar ratio) at pH 6 and 7.3 using PFG-NMR.[34−36] At pH 6, the hydrodynamic radius of the $PAP_{248-286}$/EGCG complex is similar to that of $PAP_{248-286}$ alone (~1.6 nm) (Figure 3A), indicating EGCG does not cause

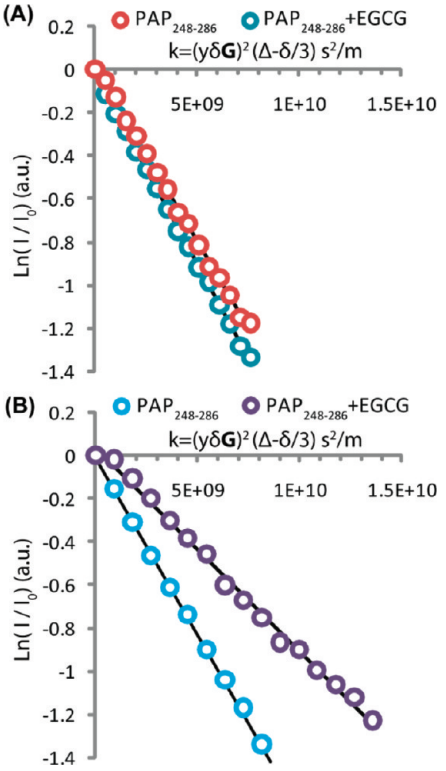

Figure 3. EGCG catalyzes the formation of small oligomeric species of $PAP_{248-286}$ at pH 7.3 but not pH 6. Normalized stimulated-echo intensity decays from STE (stimulated-echo) PFG ^{1}H NMR spectra of 215 μM $PAP_{248-286}$ with and without 215 μM EGCG at 37 °C in 50 mM potassium phosphate buffer at pH 6 (A) and pH 7.4 (B).

the immediate oligomerization of $PAP_{248-286}$ at pH 6. The high degree of correspondence between the hydrodynamic radii of $PAP_{248-286}$ and the $PAP_{248-286}$/EGCG complex is also an indication that the size of the $PAP_{248-286}$/EGCG complex is either similar to that of the $PAP_{248-286}$ monomer or that EGCG does not bind the monomeric form of $PAP_{248-286}$ with a high affinity at pH 6.

While the addition of EGCG had little discernible effect on the hydrodynamic radius of $PAP_{248-286}$ at pH 6, at pH 7.3, a white precipitate immediately formed upon the addition of EGCG. However, a detectable signal from the $PAP_{248-286}$/EGCG complex could be determined from the supernatant solution. The hydrodynamic radius of the complex formed at pH 7.3 (~3.6 nm) is substantially larger than that of $PAP_{248-286}$ alone (~1.6 nm, Figure 3B), suggesting EGCG catalyzes the fast formation of small oligomeric complexes of $PAP_{248-286}$ at pH 7.3 but not at 6.

EGCG Binds near the 251−257 and 269−277 Regions of Monomeric $PAP_{248-286}$. To investigate possible binding of EGCG to the monomeric form of $PAP_{248-286}$ and to identify target sites on the $PAP_{248-286}$ molecule, we carried out binding studies using NMR experiments. It has previously been reported that EGCG binds randomly to exposed sites on the backbone of α-synuclein and calcitonin,[14,36] which was conjectured to be a mode of binding for most amyloid proteins.[14]

dx.doi.org/10.1021/jp2121577 | J. Phys. Chem. B 2012, 116, 3650−3658

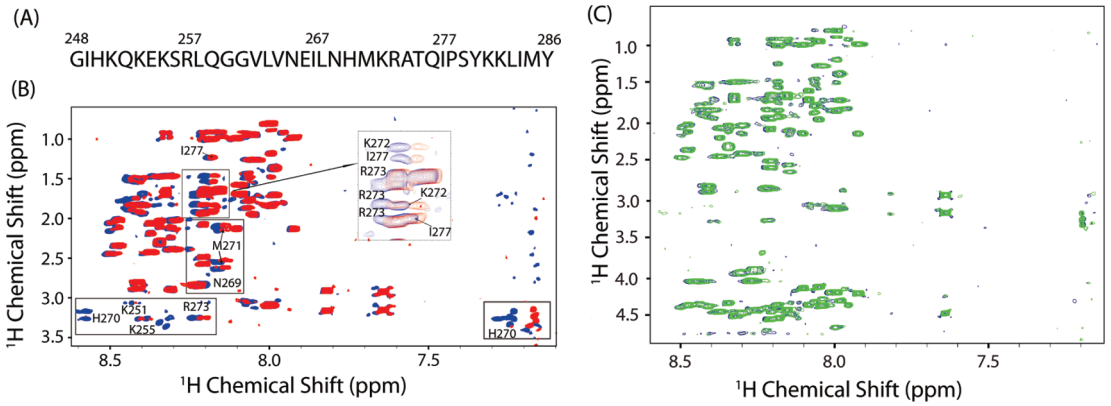

Figure 4. EGCG interacts with specific residues of $PAP_{248-286}$; GC minimally interacts with $PAP_{248-286}$. (A) Amino acid sequence of $PAP_{248-286}$ peptide. (B) Overlaid 2D $^1H-^1H$ TOCSY spectra of $PAP_{248-286}$ alone (blue) and EGCG bound to peptide (red, 1:1 molar ratio). (C) Overlaid 2D $^1H-^1H$ TOCSY spectra of GC bound to $PAP_{248-286}$ (green, 1:1 molar ratio) and $PAP_{248-286}$ alone (blue).

The addition of EGCG at 1:1 molar ratio at pH 6 caused significant broadening of resonances and substantial chemical shift perturbations for many of the residues in the 2D $^1H-^1H$ TOCSY spectrum of $PAP_{248-286}$ (Figure 4B). This finding confirms that EGCG can bind to $PAP_{248-286}$ in the monomeric state and that the interaction involves considerable involvement of the side chain atoms of $PAP_{248-286}$. The distribution of changes is not uniform and shows larger effects for particular amino acid types and regions of the peptide. Both the backbone and side chain ^1H resonances for residues near the central region of the peptide, such as N269, H270, M271, K272, R273, and I277, displayed a considerable shift after binding EGCG. The N-terminal region, particularly K251, Q252, K253, and K255, is similarly affected. The hydrophobic center of the peptide, proposed to be a spot of amyloid initiation,[37,38] was relatively unaffected. The distribution of amino acid type is similarly nonuniform, with positively charged residues (lysines, arginine, and histidine) along with methionine showing the strongest interaction. The interaction of the positively charged side chains with EGCG may reflect the formation of a salt bridge between EGCG and $PAP_{248-286}$ (two of the phenolic groups of EGCG have pK_a values near 7);[39] however, we have no direct evidence of such an interaction.

By contrast, GC, which is not an effective SEVI inhibitor,[12] did not show substantial changes in the $^1H-^1H$ TOCSY spectrum (Figure 4C). In contrast to the substantial changes seen in the $^1H-^1H$ TOCSY spectrum of EGCG/$PAP_{248-286}$, the side chain resonances of $PAP_{248-286}$ are almost unaltered by the addition of GC, indicating that GC does not have a significant interaction with the side chains of $PAP_{248-286}$.

Initial attempts at obtaining a 2D $^1H-^1H$ TOCSY spectrum of a 1:1 EGCG/$PAP_{248-286}$ complex at pH 7.3 resulted in the rapid formation of a white precipitate followed by the formation of a brown solid. EGCG alone has a high propensity to oxidize at pH 7.3 and forms a brownish solution in the absence of $PAP_{248-286}$. This is likely the result of auto-oxidation and aggregation of EGCG, which increases with the basicity of the solution between pH 4 and 8.[40]

EGCG Forms a Tightly Bound $PAP_{248-286}$/EGCG Quinone Complex after Prolonged Incubation. The NMR results show that the residues affected by EGCG binding were not randomly distributed but primarily concentrated among Lys, His, Arg, and Met residues. Both EGCG and GC are known to react with the nucleophilic side chains of proteins by Schiff-base or Michelson addition.[27] The formation of a precipitate when EGCG was added to $PAP_{248-286}$ at high concentrations suggests the formation of covalently cross-linked products may occur, as has previously been directly detected for other flavonoids in the presence of α-synuclein and with EGCG in the presence of nonamyloidogenic proteins and peptides.[27,41,42]

We first tested this possibility by a NBT staining assay, which allows the detection of SDS stable, covalently or tightly bound $PAP_{248-286}$/EGCG complexes.[26] In the NBT assay, the protein is first electrophoresed by SDS-PAGE than electroblotted into a membrane submerged in a solution containing NBT and glycine. EGCG reacts with glycine, generating a superoxide ion which reduces NBT to formazon, generating a purple spot on the membrane.[26] If EGCG is weakly bound in a conformation that is not SDS-stable, EGCG is not retained on the membrane and the formazon diffuses away during the washing step. A purple band migrating at ~4.5 kDa was detected when $PAP_{248-286}$ was incubated with EGCG at pH 7.3 for 2 days at RT, indicating a strong SDS-resistant association with EGCG (Figure 5A, lane 4). A corresponding band was not detected in the absence of EGCG (Figure 5A, lane 3) or, interestingly, when $PAP_{248-286}$ was incubated with EGCG at pH 6 under these conditions (Figure 5A, lane 2). Since these conditions roughly mirror those employed in the NMR experiment, the absence of a positive NBT-staining test at pH 6 indicates that the initial EGCG/$PAP_{248-286}$ complex observed by NMR is not likely to be formed by covalent attachment of ECGC to $PAP_{248-286}$. However, purple bands indicating the formation of a SDS-stable EGCG/$PAP_{248-286}$ complex at pH 6 became evident after a longer incubation time (2 weeks at 4 °C, Figure 5B, lane 3) but were not detected for GC (Figure 5B, lane 4).

To confirm the existence of a covalently bound complex, $PAP_{248-286}$ was incubated with EGCG or GC for 3 days at room temperature and then analyzed by ESI-MS. A 5-fold molar excess of EGCG and GC was used to improve sensitivity. In the absence of EGCG or GC, the mass chromatogram of $PAP_{248-286}$ showed a major peak at m/z = 4550.6 and a minor peak (~10% of the total) at 4566.6 that most likely corresponds to the oxidation of M271 (Figure S3A and B, Supporting Information). In the presence of EGCG, the mass chromatogram showed an additional peak at m/z = 5009.6 that could be assigned to the peptide/EGCG complex (Figure S3C and D, Supporting Information). The intensity of the peak for the EGCG/peptide complex comprised about 35% of the total and was not affected by the pH of incubation, suggesting an equilibrium for the formation of the $PAP_{248-286}$/EGCG

dx.doi.org/10.1021/jp2121577 | J. Phys. Chem. B 2012, 116, 3650–3658

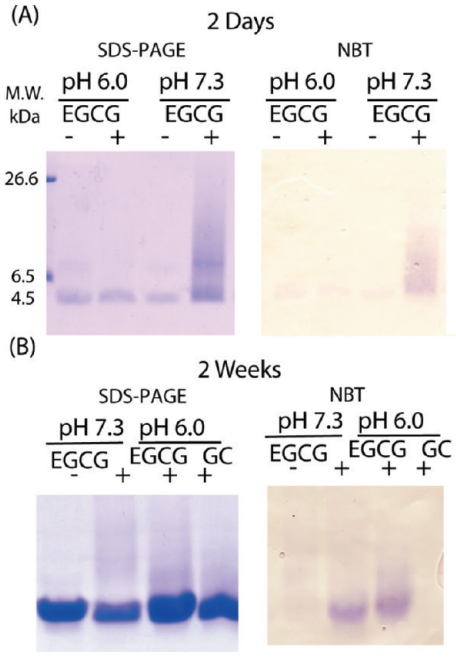

Figure 5. The formation of a tightly bound EGCG/$PAP_{248-286}$ complex is faster at pH 7.3 than at pH 6. SDS-PAGE gel (left) and NBT stained membrane (right) of $PAP_{248-286}$ alone (indicated as -) and EGCG-bound (1:5 $PAP_{248-286}$/EGCG ratio) (indicated as +) at pH 6.0 and 7.3 after 2 days of incubation at room temperature (A) and 2 weeks of incubation at 4 °C (B). The presence of a purple band after NBT staining indicates the formation of a SDS stable complex.

complex was reached after 3 days for both pH values when incubated with a 5-fold excess of EGCG. The intensity of the peak for the GC/peptide complex (m/z = 4857) is significantly weaker than that of EGCG (~10% compared to 35% for EGCG), indicating complex formation is more strongly favored for EGCG than GC (Figure S3E and F, Supporting Information). In summary, the NBT staining and ESI-MS experiments suggest the binding of EGCG to $PAP_{248-286}$ is a multistep process with covalent attachment of EGCG occurring over a period of days.

Lysine Residues Are Critical for the Interaction of $PAP_{248-286}$ and EGCG. 2D $^1H-^1H$ TOCSY and NOESY solution NMR experiments revealed the effect of EGCG on $PAP_{248-286}$ is not random but is instead heavily concentrated on the six lysines present. To examine the role of lysine in EGCG binding in more detail, we acetylated the lysine sites of $PAP_{248-286}$ by reaction with excess acetic anhydride (ESI-MS result is shown in Figure S4, Supporting Information). In the absence of EGCG, lysine-blocked $PAP_{248-286}$ formed a sparse network of thin short fibers (Figure 6A) after incubating for 1 week at pH 8. In the presence of 5 mol equiv of EGCG, a similar network of thin short fibers can be seen in the lysine-blocked $PAP_{248-286}$ sample (Figure 6B). From these results, it is apparent that acetylation of the lysine of $PAP_{248-286}$ largely blocks the inhibiting effect of EGCG on $PAP_{248-286}$ amyloid formation. To see if lysine residues are also essential for the formation of the $PAP_{248-286}$ covalent complex, lysine-blocked $PAP_{248-286}$ was incubated with EGCG for 2 days at pH 8.0 and the NBT assay performed. Bands corresponding to a tightly bound $PAP_{248-286}$/EGCG complex were not observed for the lysine-blocked samples but were observed for corresponding

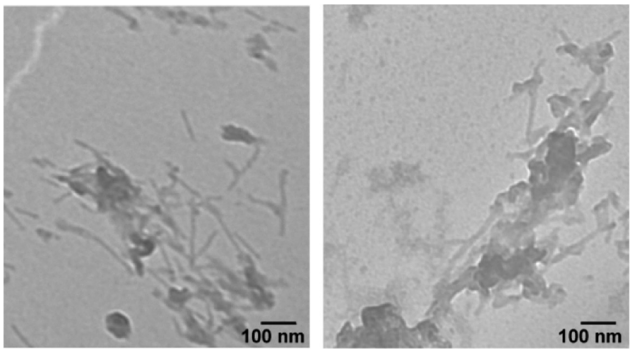

Figure 6. Lysine residues are critical for inhibition of amyloid formation by EGCG. TEM images of lysine blocked $PAP_{248-286}$ after 1 week of incubation at pH 8 (left) and 1 week of incubation at pH 8 with 5 mol equiv of EGCG (right).

non-lysine-blocked control samples (Figure 7B, lane 6), suggesting lysine's involvement in cross-linking with EGCG as well.

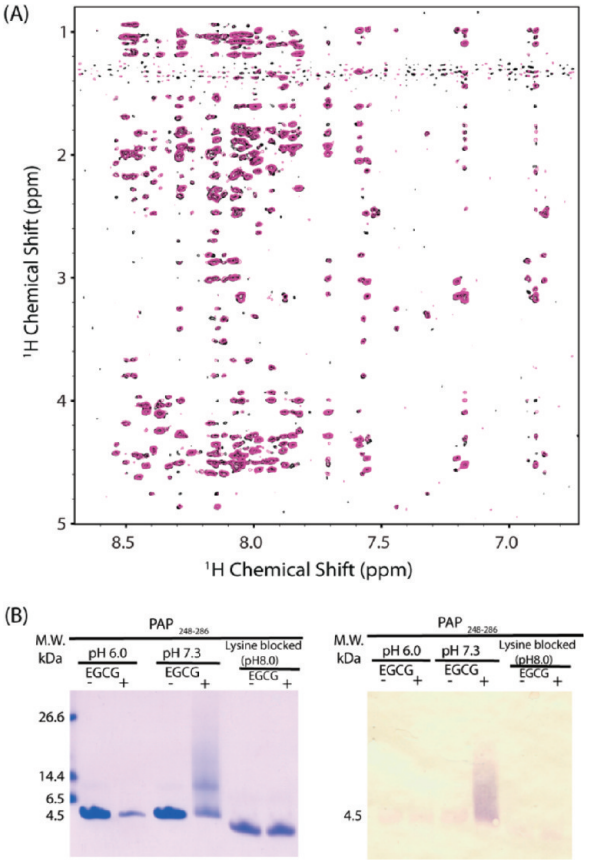

Figure 7. Lysine residues are critical for EGCG binding. (A) Overlaid 2D $^1H-^1H$ NOESY spectra of EGCG incubated with $PAP_{248-286}$ bound to 400 mM SDS (magenta) and $PAP_{248-286}$ in 400 mM SDS alone (black). The absence of any significant shifts suggests residues essential for binding are occluded when $PAP_{248-286}$ is bound to SDS. (B) SDS-PAGE gel (top) and NBT stained membrane (bottom) of $PAP_{248-286}$ alone and EGCG bound at pH 6.0 (left) and 7.3 (center) and with the lysine blocked by acetic anhydride (pH 8) (right). The absence of a purple band in the sample with the lysines blocked indicates the ε-NH_2 groups of lysine are essential for the formation of a tightly bound EGCG/$PAP_{248-286}$ complex.

The absence of perturbations in the NMR spectra of $PAP_{248-286}$ upon the addition of EGCG after it has been bound to SDS

dx.doi.org/10.1021/jp2121577 | J. Phys. Chem. B 2012, 116, 3650–3658

provided additional evidence for the importance of lysines in the interaction of $PAP_{248-286}$ with EGCG. In SDS micelles, $PAP_{248-286}$ adopts a disordered structure on the surface of the micelle.[38] While most of the backbone sites are exposed to solvent and available for binding in SDS, the lysine side chains are buried within the micelle and shielded from interaction with EGCG.[38] No changes in either the side chain or amide backbone resonances were apparent in the $^1H-^1H$ TOCSY spectrum of $PAP_{248-286}$ in 400 mM SDS at pH 6 upon the addition of EGCG (Figure 7A). The absence of significant changes in the $^1H-^1H$ TOCSY spectrum and the absence of NBT-positive bands when the lysine side chains are blocked are both strong indications that lysine residues are indeed essential for the formation of a tightly bound complex between $PAP_{248-286}$ and EGCG.

DISCUSSION

Besides $PAP_{248-286}$, EGCG both inhibits amyloid fiber formation and destabilizes existing amyloid fibers formed from a variety of other amyloid proteins including α-synuclein, $A\beta_{1-42}$ and $A\beta_{1-40}$, IAPP, transthyretin, human and yeast prions, lysozyme, human calcitonin, κ-casein, and tau.[19,20,36,43−46] The molecular mechanism by which this is accomplished is not yet clear. Initially, it was proposed that EGCG diverts the normal aggregation pathway of amyloidogenic proteins into the formation of spherical unstructured aggregates, which form a nontoxic, off-pathway state that does not progress further to the amyloid form.[14,16,46] On a molecular level, EGCG has been proposed to bind to the exposed backbone of the unfolded regions of proteins, presumably blocking the association of these aggregation prone regions.[14]

The evidence for this mechanism primarily comes from studies of α-synuclein and $A\beta_{1-42}$.[14] NBT staining showed a strong, SDS stable, association of EGCG with both of these peptides and with denatured BSA but not with control proteins that were natively folded.[14] Further, NMR studies of α-synuclein showed changes in the HSQC (heteronuclear single quantum coherence) spectrum induced by EGCG were concentrated in the flexible C-terminus of the peptide, and not in the more ordered N-terminus.[14] The changes were not concentrated on a particular type of residue, suggesting nonspecific binding to the peptide backbone rather than specific binding to the elements of the side chains.[14]

On the basis of the apparent generality of amyloid inhibition by EGCG, the formation of off-pathway aggregates by nonspecific binding of EGCG to exposed backbone sites was proposed as a generic mechanism for amyloid inhibition by EGCG.[14] However, more recent data suggests this mechanism is not entirely general. The crystal structure of EGCG bound to the tetrameric form of transthyretin reveals EGCG binds at specific sites in transthyretin, interacting with the folded transthyretin tetramer by a combination of specific hydrophobic and hydrophilic contacts with side chains and interactions with exposed amide backbones.[47] EGCG has also been shown to interact with the helical native structure of the human prion protein and with nonflexible regions of κ-casein,[44] suggesting unfolded conformations are not a strict necessity for EGCG binding, in agreement with reports of EGCG binding to multiple natively folded nonamyloidogenic proteins.[48] Similarly, NMR studies have suggested EGCG primarily stabilizes the monomeric structure of human calcitonin rather than redirecting the aggregation to amorphous aggregates.[36]

In striking contrast to the apparently random distribution of residues affected by EGCG in α-synuclein and $A\beta_{1-42}$,[14] EGCG primarily interacts with $PAP_{248-286}$ through the side chains of a specific set of residues. Chemical shift perturbations are concentrated at two clusters of residues, the first near the N-terminus and the second closer to the center of the peptide (Figure 4B). Pronounced changes in particular were detected for the positively charged side chains of lysines, suggesting a specific interaction of EGCG with this residue. The strong association of EGCG with lysine was confirmed by the absence of a strong interaction with $PAP_{248-286}$ when the lysine residues of $PAP_{248-286}$ were chemically blocked (Figure 7B, lane 6). Further evidence for the importance of lysine in EGCG binding was provided by the NMR spectra of EGCG titrated to $PAP_{248-286}$ bound to SDS micelles. In the SDS micelle, the positively charged lysine side chains of $PAP_{248-286}$ are strongly bound to the negatively charged headgroups of SDS and are therefore not available for EGCG binding, while the remainder of the protein is disordered and exposed to solvent.[38] Virtually no change in the spectrum was observed for $PAP_{248-286}$ bound to SDS when EGCG was added, indicating association of EGCG with lysine is essential for binding (Figure 7A).

The changes in chemical shift of the initial $PAP_{248-286}$/ECGC at pH 6 are reflective of a relatively weak interaction with EGCG, with exchange occurring on a fast time scale, similar to what has been observed for the initial complexes of EGCG with the amyloidogenic proteins α-synuclein and MSP2.[14,43] The formation of an initially weak complex is consistent with the absence of a color reaction with NBT when $PAP_{248-286}$ is incubated for 2 days at pH 6 (Figure 5A, lane 2), indicating complex formation is initially reversible and weak enough to be removed by SDS. By contrast, NBT reacts immediately with the complex of $PAP_{248-286}$ and ECGC formed at pH 7.3 (Figure 5B, lane 4). PFG NMR shows that, while the hydrodynamic radius of the $PAP_{248-286}$/ECGC complex formed at pH 6 is similar to that of $PAP_{248-286}$ alone, the hydrodynamic radius of the complex formed at pH 7.4 is substantially larger, reflecting the oligomerization of the peptide induced by EGCG (Figure 3). Oxidized EGCG is known to form covalently cross-linked complexes with proteins, a process influenced by a number of factors including pH, temperature, oxygen, and transition metal concentrations, and the concentration of EGCG.[42,49,50] Methionine residues in particular are easily oxidized by EGCG, generating hydrogen peroxide and a reactive quinone product.[27] Once oxidized to the reactive quinone form, EGCG is subject to attack by the nucleophilic side chains of lysine, histidine, and arginine residues as well as the N-terminus of the peptide to yield an acid-labile Schiff base.[27,42,51,52] It should be noted, however, that the formation of a covalent EGCG/$PAP_{248-286}$ complex is apparently not an absolute prerequisite for efficient inhibition of amyloid formation, as amyloid formation was inhibited by EGCG at acidic pH where formation of the covalent complex is disfavored and occurs slowly, in contrast to the relatively rapid disaggregation of amyloid fibrils observed by TEM. The eventual formation of a covalent complex is apparently also not sufficient to inhibit amyloid fiber formation, as the related compound GC does not have a strong inhibitory effect on amyloid formation even though it does slowly form a covalent or a noncovalent tightly bound complex (albeit less efficiently than EGCG) (see Figure S3, Supporting Information). Instead, the greater ability of EGCG to inhibit amyloid formation compared to GC is most likely due to a stronger initial association, as reflected in the

stronger chemical shift perturbations observed in the NMR spectra of the EGCG/$PAP_{248-286}$ complex (Figure 4).

CONCLUSION

Our results show that EGCG inhibits SEVI fibril formation at both neutral and acidic pH in good agreement with biophysical, biochemical, and genetic data for other amyloidogenic proteins. However, the binding mechanism of EGCG to $PAP_{248-286}$ deviates substantially from the proposed general model for polyphenols binding to amyloid proteins. Instead of driving the formation of large amorphous off-pathway aggregates, EGCG binds to $PAP_{248-286}$ in the monomeric form, disaggregating fibrils completely to small EGCG/$PAP_{248-286}$ complexes. In addition, binding appears to be driven by interactions with the side chains of $PAP_{248-286}$ with EGCG, rather than interactions with exposed backbone sites as previously proposed. These differences may be due to the unusually high charge and low overall hydrophobicity of the $PAP_{248-286}$ protein when compared to most other amyloid proteins.

While the precise mechanism by which EGCG inhibits SEVI amyloid formation is uncertain, the delay between the time in which perturbations in the NMR spectra are detected and time in which NBT staining indicates the formation of a tightly bound complex suggests the binding of EGCG to $PAP_{248-286}$ is a multistep process.[41] In the first step, a weakly bound, noncovalent complex is formed, most likely by hydrogen bonding and hydrophobic interactions.[53,54] In the next step, a covalent complex is formed by Schiff base addition after the generation of a reactive quinone complex by autoxidation of EGCG. Further studies aimed at characterizing the interaction of EGCG with the SEVI fibrillar form of $PAP_{248-286}$ are in progress.

ASSOCIATED CONTENT

Supporting Information

Complete reference 2, kinetics of amyloid formation of $PAP_{248-286}$ at pH 6 and 7.3 by ThT fluorescence (Figure S1), TEM images of $PAP_{248-286}$ incubated with GC (Figure S2), ESI-MS of $PAP_{248-286}$ at pH 6 and 7.3 with EGCG (Figure S3), and ESI-MS of lysine-blocked $PAP_{248-286}$ (Figure S4). This material is available free of charge via the Internet at http://pubs.acs.org.

AUTHOR INFORMATION

Corresponding Author

*Phone: 734-647-6572. Fax: 734-764-3323. E-mail: ramamoor@umich.edu.

Notes

The authors declare no competing financial interest.

ACKNOWLEDGMENTS

This study was supported by research funds from NIH (DK078885 and RR023597 to A.R.).

REFERENCES

(1) Doncel, G. F.; Joseph, T.; Thurman, A. R. *Am. J. Reprod. Immunol.* **2011**, *65*, 292−301.
(2) Easterhoff, D.; DiMaio, J. T. M.; Doran, T. M.; Dewhurst, S.; Nilsson, B. L. *Biophys. J.* **2011**, *100*, 1325−1334.
(3) Munch, J.; et al. *Cell* **2007**, *131*, 1059−1071.
(4) Roan, N. R.; Munch, J.; Arhel, N.; Mothes, W.; Neidleman, J.; Kobayashi, A.; Smith-McCune, K.; Kirchhoff, F.; Greene, W. C. *J. Virol.* **2009**, *83*, 73−80.
(5) Kim, K. A.; Yolamanova, M.; Zirafi, O.; Roan, N. R.; Staendker, L.; Forssmann, W. G.; Burgener, A.; Dejucq-Rainsford, N.; Hahn, B. H.; Shaw, G. M.; Greene, W. C.; Kirchhoff, F.; Munch, J. *Retrovirology* **2010**, *7*, 55−67.
(6) Roan, N. R.; Sowinski, S.; Munch, J.; Kirchhoff, F.; Greene, W. C. *J. Biol. Chem.* **2010**, *285*, 1861−1869.
(7) Wurm, M.; Schambach, A.; Lindemann, D.; Hanenberg, H.; Standker, L.; Forssmann, W. G.; Blaszczyk, R.; Horn, P. A. *J. Gene Med.* **2010**, *12*, 137−146.
(8) Hong, S. H.; Klein, E. A.; Das Gupta, J.; Hanke, K.; Weight, C. J.; Nguyen, C.; Gaughan, C.; Kim, K. A.; Bannert, N.; Kirchhoff, F.; Munch, J.; Silverman, R. H. *J. Virol.* **2009**, *83*, 6995−7003.
(9) Brender, J. R.; Hartman, K.; Gottler, L. M.; Cavitt, M. E.; Youngstrom, D. W.; Ramamoorthy, A. *Biophys. J.* **2009**, *97*, 2474−2483.
(10) Capule, C. C.; Brown, C.; Olsen, J. S.; Dewhurst, S.; Yang, J. *J. Am. Chem. Soc.* **2012**, *134*, 905−908.
(11) Olsen, J. S.; Brown, C.; Capule, C. C.; Rubinshtein, M.; Doran, T. M.; Srivastava, R. K.; Feng, C.; Nilsson, B. L.; Yang, J.; Dewhurst, S. *J. Biol. Chem.* **2010**, *285*, 35488−35496.
(12) Hauber, I.; Hohenberg, H.; Holstermann, B.; Hunstein, W.; Hauber, J. *Proc. Natl. Acad. Sci. U.S.A.* **2009**, *106*, 9033−9038.
(13) Porat, Y.; Abramowitz, A.; Gazit, E. *Chem. Biol. Drug Des.* **2006**, *67*, 27−37.
(14) Ehrnhoefer, D. E.; Bieschke, J.; Boeddrich, A.; Herbst, M.; Masino, L.; Lurz, R.; Engemann, S.; Pastore, A.; Wanker, E. E. *Nat. Struct. Mol. Biol.* **2008**, *15*, 558−566.
(15) Ladiwala, A. R. A.; Lin, J. C.; Bale, S. S.; Marcelino-Cruz, A. M.; Bhattacharya, M.; Dordick, J. S.; Tessier, P. M. *J. Biol. Chem.* **2010**, *285*, 24228−24237.
(16) Bieschke, J.; Russ, J.; Friedrich, R. P.; Ehrnhoefer, D. E.; Wobst, H.; Neugebauer, K.; Wanker, E. E. *Proc. Natl. Acad. Sci. U.S.A.* **2010**, *107*, 7710−7715.
(17) Ladiwala, A. R.; Dordick, J. S.; Tessier, P. M. *J. Biol. Chem.* **2010**, *286*, 3209−3218.
(18) Stefani, M. *FEBS J.* **2010**, *277*, 4602−4613.
(19) Meng, F. L.; Abedini, A.; Plesner, A.; Verchere, C. B.; Raleigh, D. P. *Biochemistry* **2010**, *49*, 8127−8133.
(20) Ferreira, N.; Cardoso, I.; Domingues, M. R.; Vitorino, R.; Bastos, M.; Bai, G. Y.; Saraiva, M. J.; Almeida, M. R. *FEBS Lett.* **2009**, *583*, 3569−3576.
(21) Mandel, S. A.; Amit, T.; Weinreb, O.; Reznichenko, L.; Youdim, M. B. H. *CNS Neurosci. Ther.* **2008**, *14*, 352−365.
(22) Goddard, T. D.; Kneller, D. G. *SPARKY 3*; University of California: San Francisco, CA, 1999.
(23) Tanner, J. E. *J. Chem. Phys.* **1970**, *52*, 2523−2526.
(24) Mills, R. *J. Phys. Chem.* **1973**, *77*, 685−688.
(25) Stejskal, E. O.; Tanner, J. E. *J. Chem. Phys.* **1965**, *42*, 288−292.
(26) Paz, M. A.; Fluckiger, R.; Boak, A.; Kagan, H. M.; Gallop, P. M. *J. Biol. Chem.* **1991**, *266*, 689−692.
(27) Cao, D.; Zhang, Y. J.; Zhang, H. H.; Zhong, L. W.; Qian, X. H. *Rapid Commun. Mass Spectrom.* **2009**, *23*, 1147−1157.
(28) TeviBenissan, C.; Belec, L.; Levy, M.; SchneiderFauveau, V.; Mohamed, A. S.; Hallouin, M. C.; Matta, M.; Gresenguet, G. *Clin. Diagn. Lab. Immunol.* **1997**, *4*, 367−374.
(29) Ye, Z. Q.; French, K. C.; Popova, L. A.; Lednev, I. K.; Lopez, M. M.; Makhatadze, G. I. *Biochemistry* **2009**, *48*, 11582−11591.
(30) Hudson, S. A.; Ecroyd, H.; Kee, T. W.; Carver, J. A. *FEBS J.* **2009**, *276*, 5960−5972.
(31) Chandrashekaran, I. R.; Adda, C. G.; MacRaild, C. A.; Anders, R. F.; Norton, R. S. *Arch. Biochem. Biophys.* **2011**, *513*, 153−157.
(32) Liu, K. N.; Wang, H. Y.; Chen, C. Y.; Wang, S. S. S. *Amino Acids* **2010**, *39*, 821−829.
(33) Ladiwala, A. R. A.; Dordick, J. S.; Tessier, P. M. *J. Biol. Chem.* **2011**, *286*, 3209−3218.
(34) Brender, J. R.; Nanga, R. P. R; Popovych, N.; Soong, R.; Macdonald, P. M.; Ramamoorthy, A. *Biochim. Biophys. Acta* **2011**, *1808*, 1161−1169.

(35) Soong, R.; Brender, J. R.; Macdonald, P. M.; Ramamoorthy, A. *J. Am. Chem. Soc.* **2009**, *131*, 7079−7085.
(36) Huang, R.; Vivekanandan, S.; Brender, J. R.; Abe, Y.; Naito, A.; Ramamoorthy, A. *J. Mol. Biol.* **2012**, *416*, 108−120.
(37) Sievers, S. A.; Karanicolas, J.; Chang, H. W.; Zhao, A.; Jiang, L.; Zirafi, O.; Stevens, J. T.; Munch, J.; Baker, D; Eisenberg, D. *Nature* **2011**, *475*, 96−100.
(38) Nanga, R. P. R; Brender, J. R.; Vivekanandan, S.; Popovych, N.; Ramamoorthy, A. *J. Am. Chem. Soc.* **2009**, *131*, 17972−17979.
(39) Kumamoto, M; Sonda, T.; Nagayama, K.; Tabata, M. *Biosci., Biotechnol., Biochem.* **2001**, *65*, 126−132.
(40) Zhu, Q. Y.; Zhang, A. Q.; Tsang, D.; Huang, Y.; Chen, Z. Y. *J. Agric. Food Chem.* **1997**, *45*, 4624−4628.
(41) Meng, X. Y.; Munishkina, L. A.; Fink, A. L.; Uversky, V. N. *Biochemistry* **2009**, *48*, 8206−8224.
(42) Ishii, T.; Ichikawa, T.; Minoda, K.; Kusaka, K.; Ito, S.; Suzuki, Y.; Akagawa, M.; Mochizuki, K.; Goda, T.; Nakayama, T. *Biosci., Biotechnol., Biochem.* **2011**, *75*, 100−106.
(43) Chandrashekaran, I. R.; Adda, C. G.; MacRaild, C. A.; Anders, R. F.; Norton, R. S. *Biochemistry* **2010**, *49*, 5899−5908.
(44) Hudson, S. A.; Ecroyd, H.; Dehle, F. C.; Musgrave, I. F.; Carver, J. A. *J. Mol. Biol.* **2009**, *392*, 689−700.
(45) Roberts, B. E.; Duennwald, M. L.; Wang, H.; Chung, C.; Lopreiato, N. P.; Sweeny, E. A.; Knight, M. N.; Shorter, J. *Nat. Chem. Biol.* **2009**, *5*, 936−946.
(46) He, J.; Xing, Y. F.; Huang, B.; Zhang, Y. Z.; Zeng, C. M. *J. Agric. Food Chem.* **2009**, *57*, 11391−11396.
(47) Miyata, M.; Sato, T.; Kugimiya, M.; Sho, M.; Nakamura, T.; Ikemizu, S.; Chirifu, M.; Mizuguchi, M.; Nabeshima, Y.; Suwa, Y.; Morioka, H.; Arimori, T.; Suico, M. A.; Shuto, T.; Sako, Y.; Momohara, M.; Koga, T.; Morino-Koga, S.; Yamagata, Y.; Kai, H. *Biochemistry* **2010**, *49*, 6104−6114.
(48) Maiti, T. K.; Ghosh, K. S.; Dasgupta, S. *Proteins: Struct., Funct., Bioinform.* **2006**, *64*, 355−362.
(49) Wang, R.; Zhou, W. B.; Jiang, X. H. *J. Agric. Food Chem.* **2008**, *56*, 2694−2701.
(50) Sang, S. M.; Lee, M. J.; Hou, Z.; Ho, C. T.; Yang, C. S. *J. Agric. Food Chem.* **2005**, *53*, 9478−9484.
(51) Fluckiger, R.; Woodtli, T.; Gallop, P. M. *Biochem. Biophys. Res. Commun.* **1988**, *153*, 353−358.
(52) Grelle, G.; Otto, A.; Lorenz, M.; Frank, R. F.; Wanker, E. E.; Bieschke, J. *Biochemistry* **2011**, *50*, 10624−10636.
(53) Wang, S. H.; Liu, F. F.; Dong, X. Y.; Sun, Y. *J. Phys. Chem. B* **2010**, *114*, 11576−11583.
(54) Jobstl, E.; Howse, J. R.; Fairclough, J. P. A; Williamson, M. P. *J. Agric. Food Chem.* **2006**, *54*, 4077−4081.